MD Simulations of High-dose Irradiation in Tungsten:

The Role of Peripheral Defects & Morphology

Utkarsh Bhardwaj & Manoj Warrier
CAD, BARC - Vizag, India

– Presenting at MoD-PMI - 2025 –

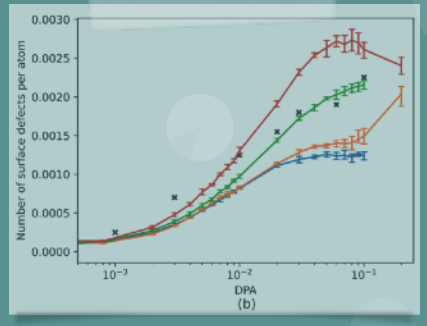

A Successive Collision Cascade Simulation

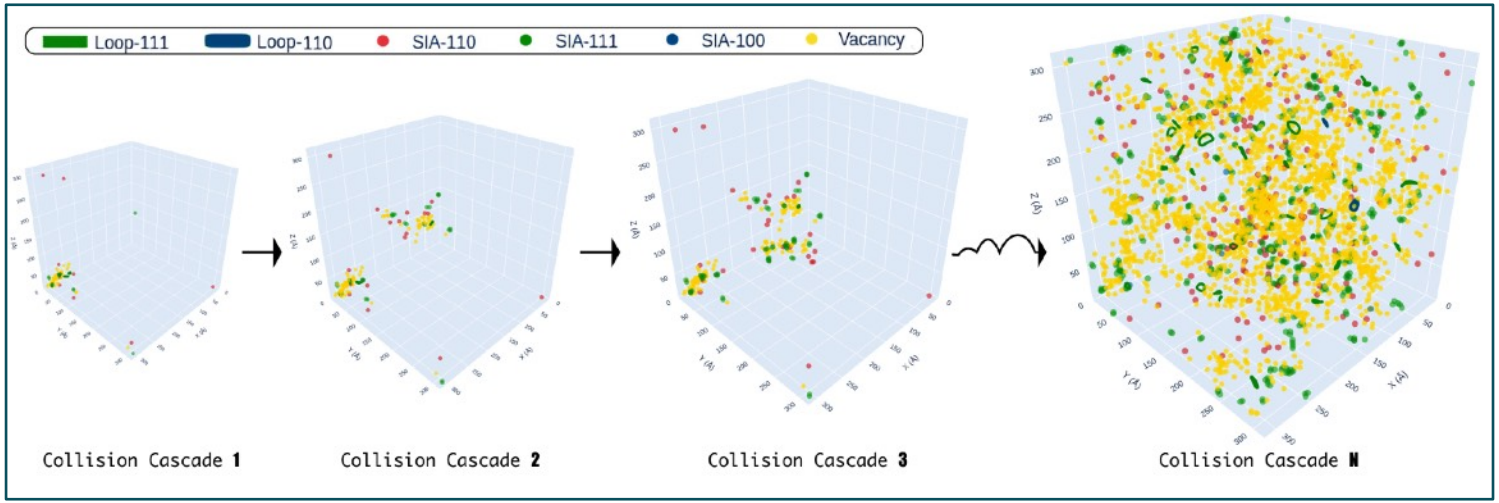

PKA Energy (keV)	IAP used	Number of PKA Launched	dpa
20	DND-BN	2500	0.11
20	SNAP	2500	0.11
50	DND-BN	2000	0.22
50	SNAP	2000	0.22

5 trials for each case
total 45000 PKA simulations

W Successive Collision Cascades Results: A Qualitative Overview

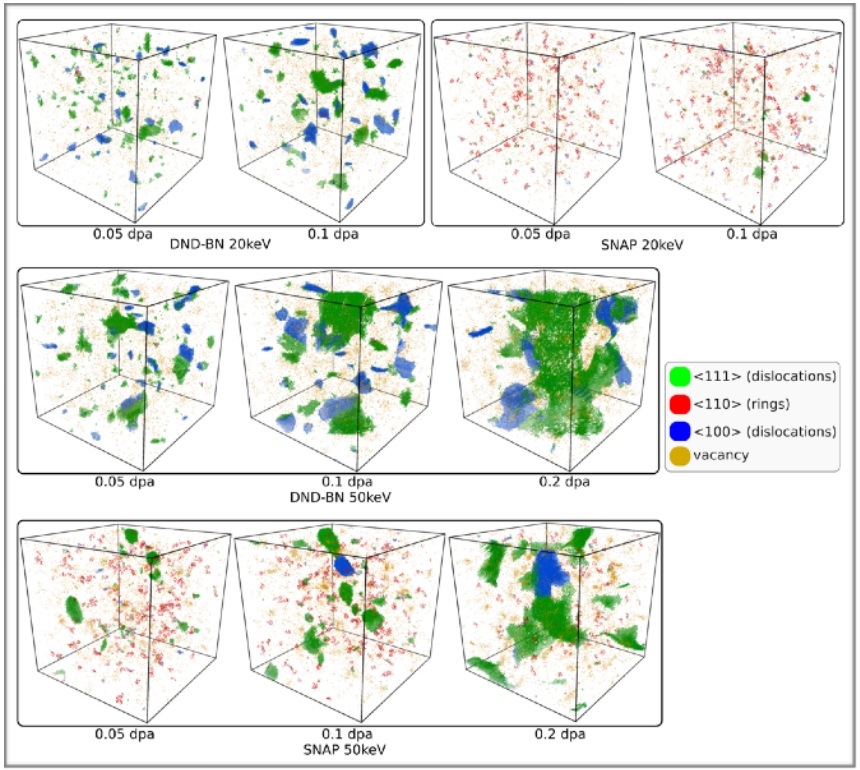

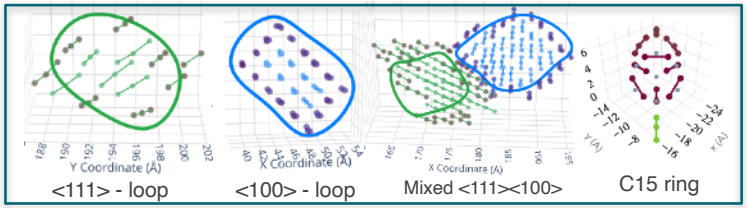

Observations:

- Higher dpa => more defects / defect sizes
- More PKA energy => more defect sizes
- SNAP => more rings
- DND-BN => more <111> & <100> loops

Both agree with experiments on:

- Presence of <111> & fewer <100> loops.
- Dislocation networks at higher dpa.

Exp. Ref [1] X.Yi et. Al. Acta Materialia 112 (2016) 105-120

Peripheral Defects

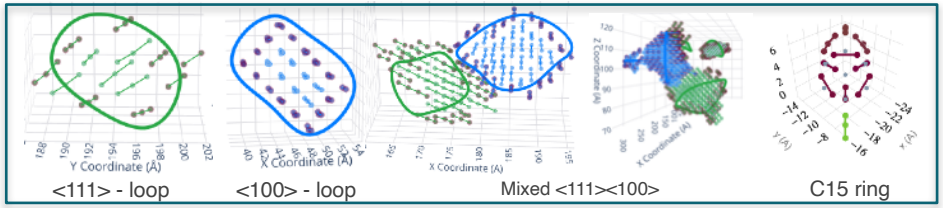

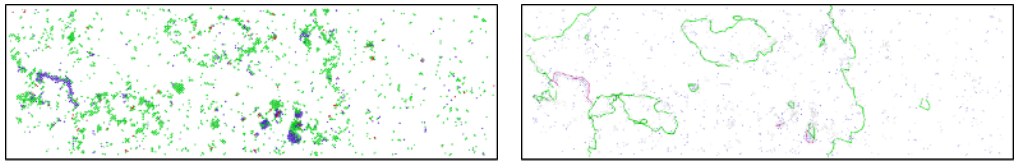

AnuVikar-ML (AviML) Model <=> Dislocation lines in DXA Ovito

- thermal diffusivity => lattice distortion
- lattice distortion => peripheral defects(p)
- TGS Experiment => peripheral defects
- p = total SIA defects - crowdions in core
- Defects in the core of a dislocation are less strained.
- The ML models trained on LAEs of defects vs non-defects inherently shows core as non-defect.

TGS Experiment Ref: A. Reza et.al. Acta Materialia 193 (2020) 270-279

Basic Properties
Number of Peripheral Defects

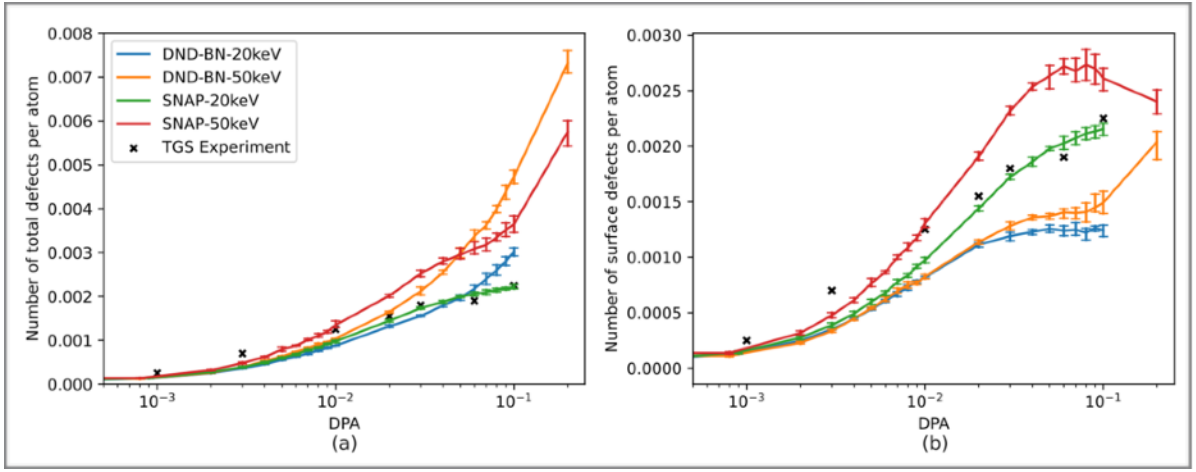

y-axis ranges are different for the two plots

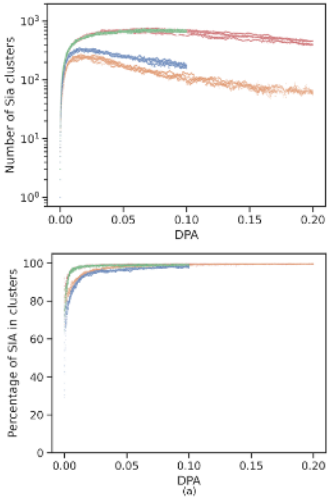

- For the peripheral defect count differences among potentials and energies are greatly reduced.
- Difference in total & peripheral defects is more where bigger loops exist (higher PKA energy, DND-BN).
- On right insets, same value of in-cluster SIAs & decreasing number of SIA clusters indicate merging of clusters.

Basic Properties

Number of Peripheral Defects With AviML

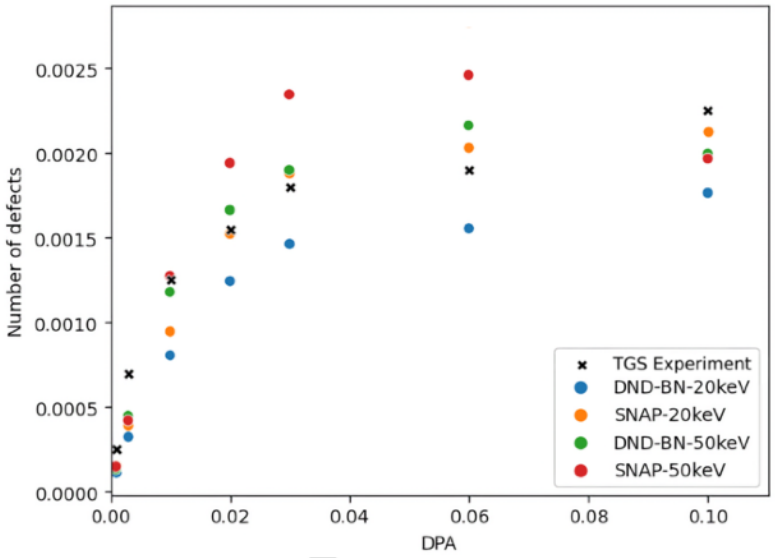

- AviML: ML model trained on the LAE of SIAs, Vacancy neighbours and orientation of SIAs
- The results show similar trends and saturation at the same level

Loop Number Density

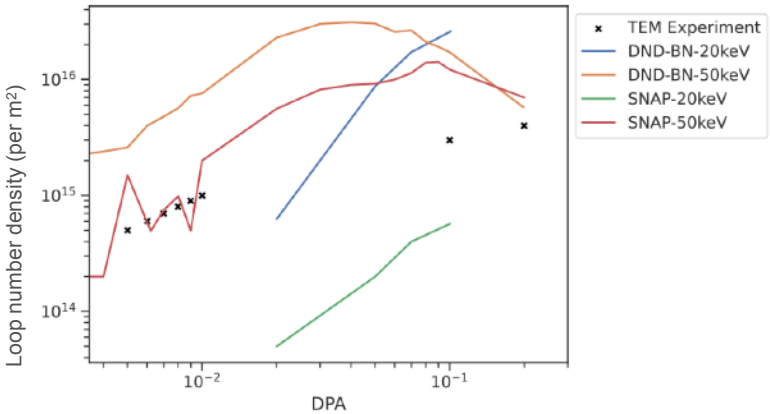

- 50 keV: loop number densities first increase up to ~0.1 dpa then decrease as loops merge.
  - This is in agreement with [2] which also shows saturation at 0.2 dpa.
- 20 keV cases are in the early stages of building up more bigger clusters; saturation expected later.
- Experimental values are from 150 keV W-ion irradiation. Higher energies may result in more number of bigger defects initially while showing lesser defects as the dislocations start to merge.

[1] X.Yi et. al. Acta Materialia 112 (2016) 105-120

[2] S.Wang et. al. Acta Materialia 244 (2023) 118578

Swelling

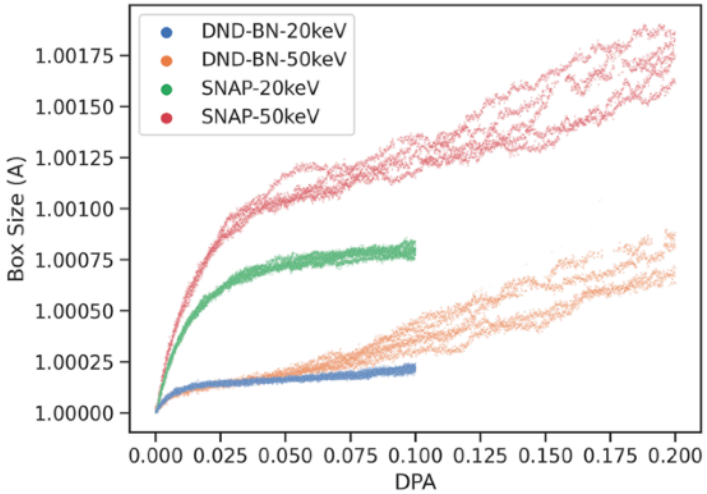

- Experimental values of 0.2 to 0.4% at different doses match better with the SNAP.

Exp. Ref [1] X.Yi et. Al. Acta Materialia 112 (2016) 105-120

Exp. Ref [2] S.Wang et. Al. Acta Materialia 244 (2023) 118578

Defect Morphology Distribution

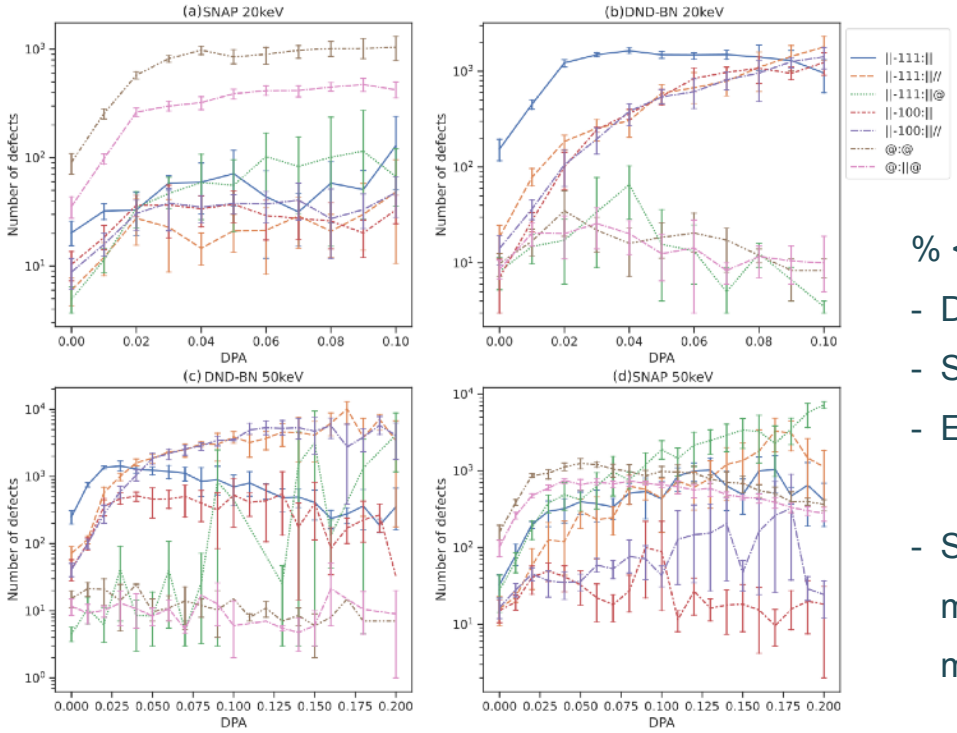

% <100> loops:

- DND-BN: ~50%
- SNAP: remains less than 25%
- Experiments: 30 - 40%

- Some experiments mention absence of mixed loops but both show those as majority at 50 keV

SaVi: Algorithm for Peripheral Defects

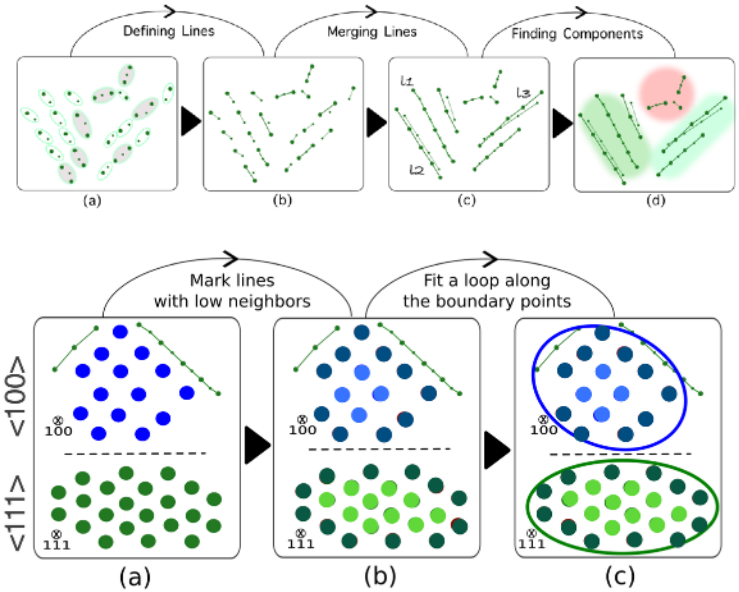

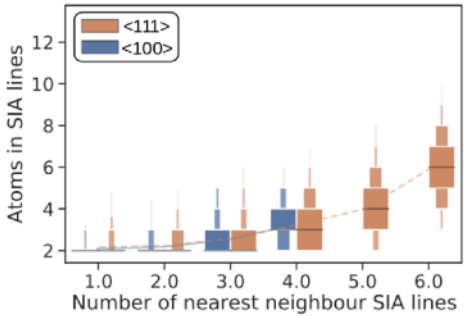

- Neighbours for a core dumbbell in <100> loop are 4 and <111> are 6.
- burgers vector direction for the dislocation is same as the direction of the crowdions/ dumbbells

U.Bhardwaj et. Com.Mat.Sci. 195 (2021) 110474

SaVi Applications and Comparison

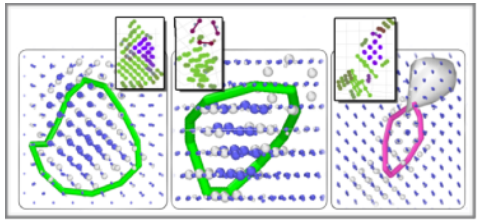

DXA vs SaVi on mixed morphology

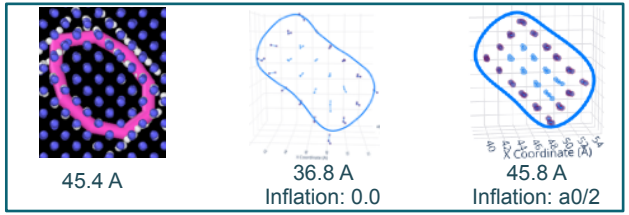

Loop lengths comparison

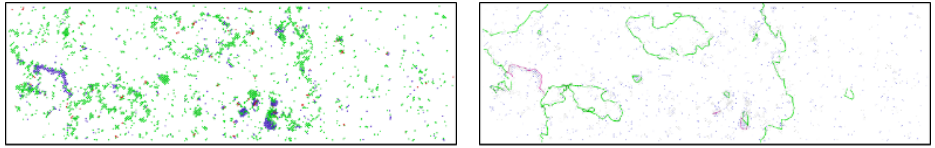

AnuVikar-ML (AviML) Model <=> Dislocation lines in DXA Ovito

- Works better with mixed morphologies
- Matches well with DXA dislocation lengths with inflation of the loop to a0/2.
- No need for full xyz file for analysis saves storage.
- O(n)log(n) time-complexity algorithm

- Boundary defects vs. Non-boundary defects aware ML models can be trained for fast, parallel and in-situ detection of boundary defects.

AnuVikar ML: AviML

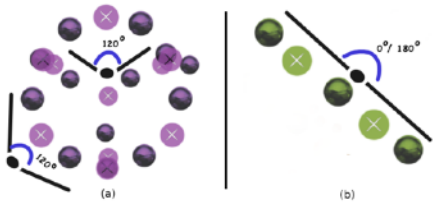

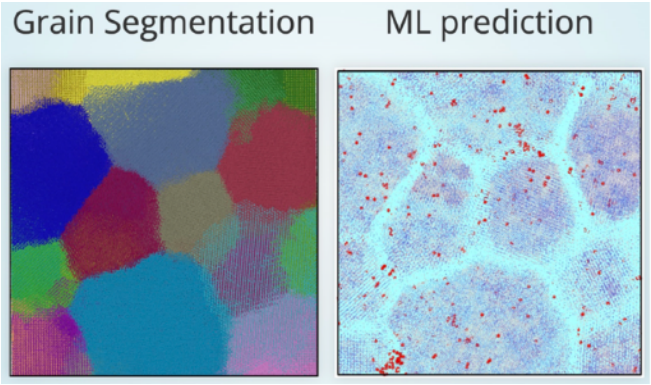

- simple features like interatomic distances and angles are enough for getting a decent accuracy on such classification.
- Classifying atoms into grain boundaries, Sia morphologies, boundary and non-boundary SIAs etc. can be done with over 90% accuracy.

U.Bhardwaj et. Com.Mat.Sci. 172 (2020) 109364

Kanad Framework

MLIP Development

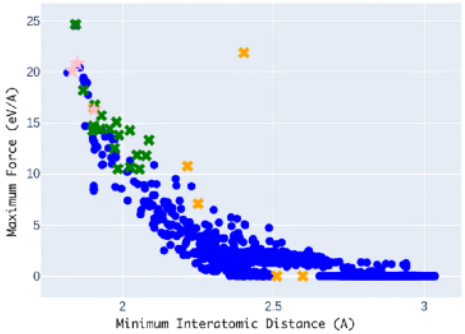

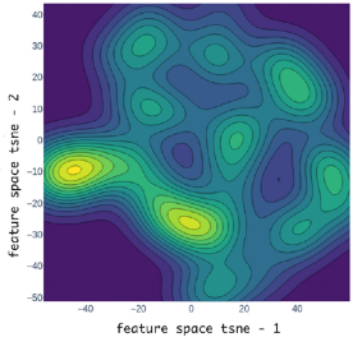

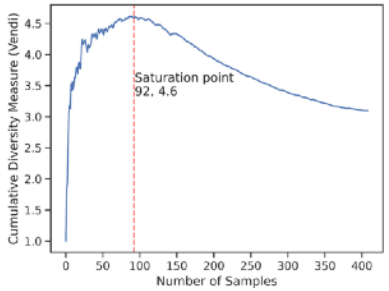

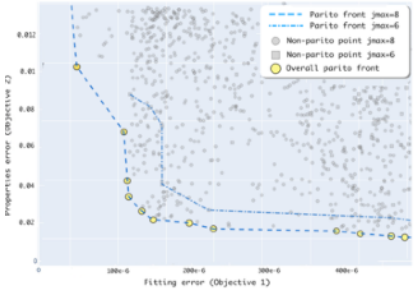

IP Validation & Comparison

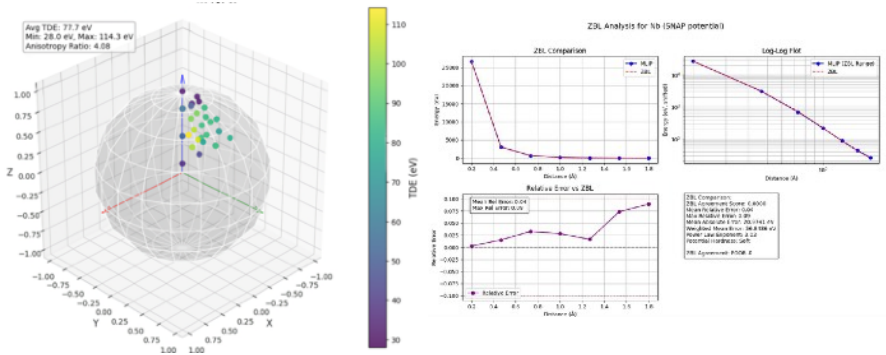

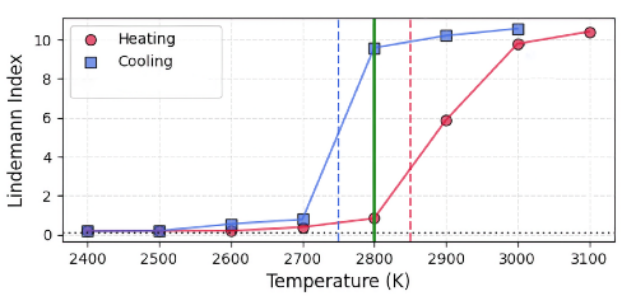

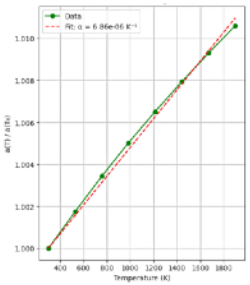

Elastic Properties

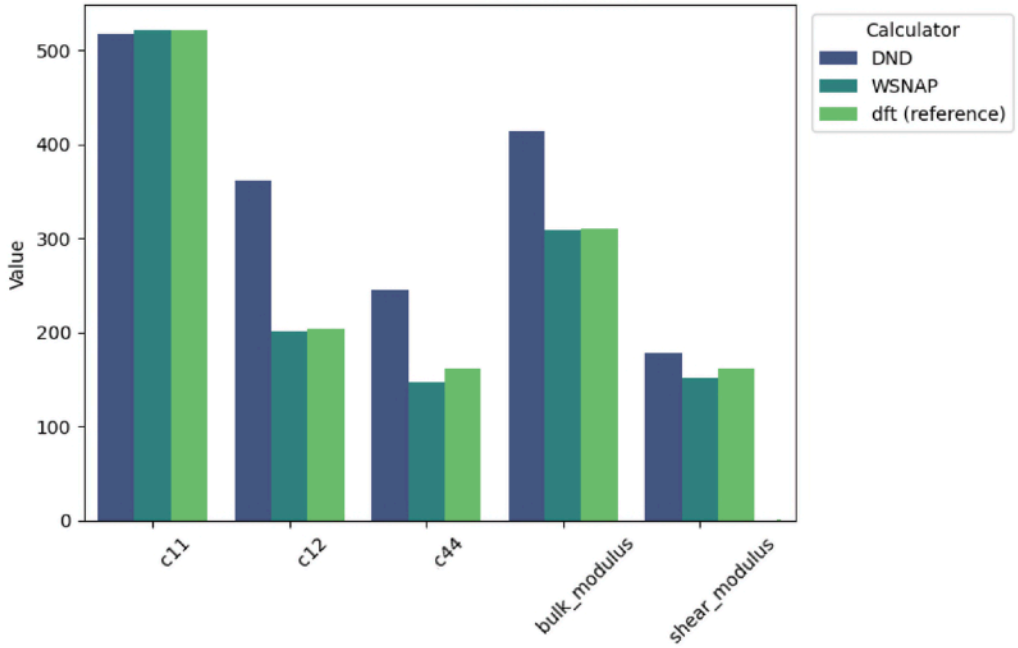

Dimer Curves & ZBL

DND-BN

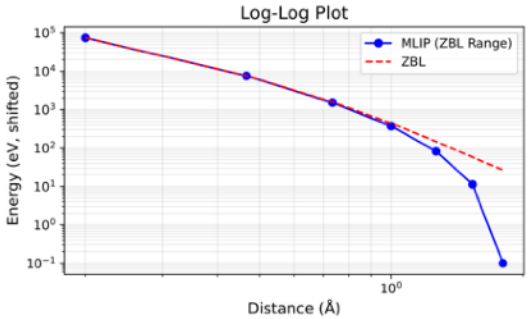

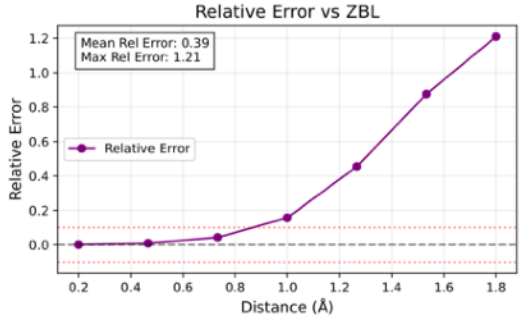

WSNAP

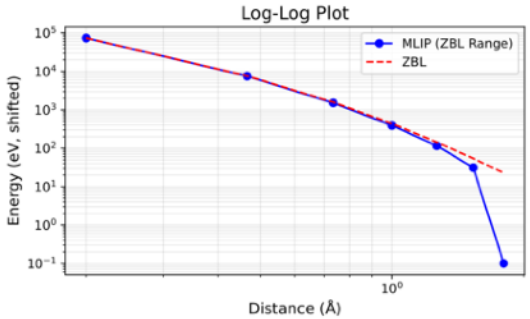

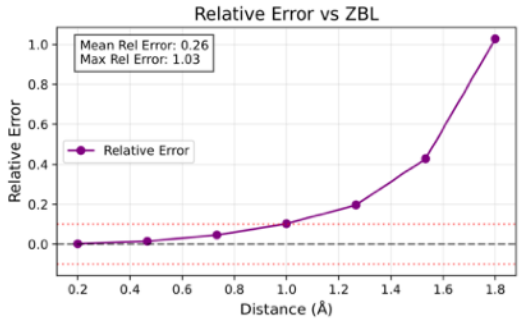

E-V Curve & dE/dV

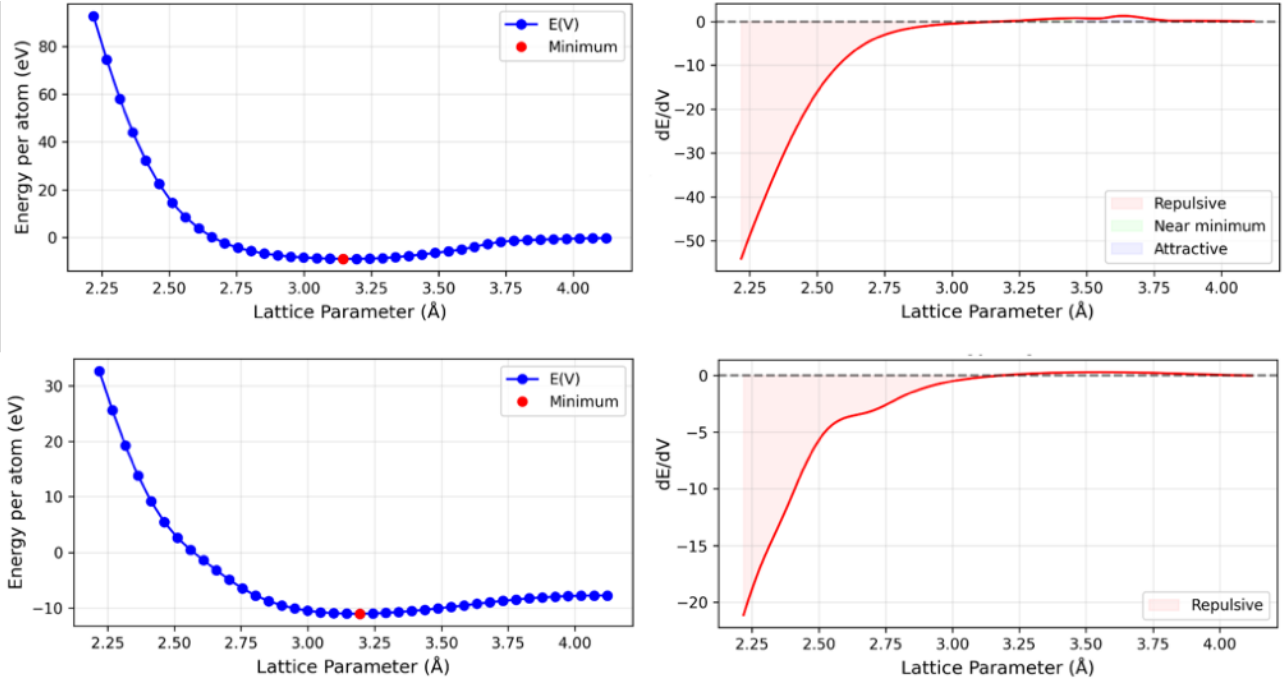

Thermal Expansion

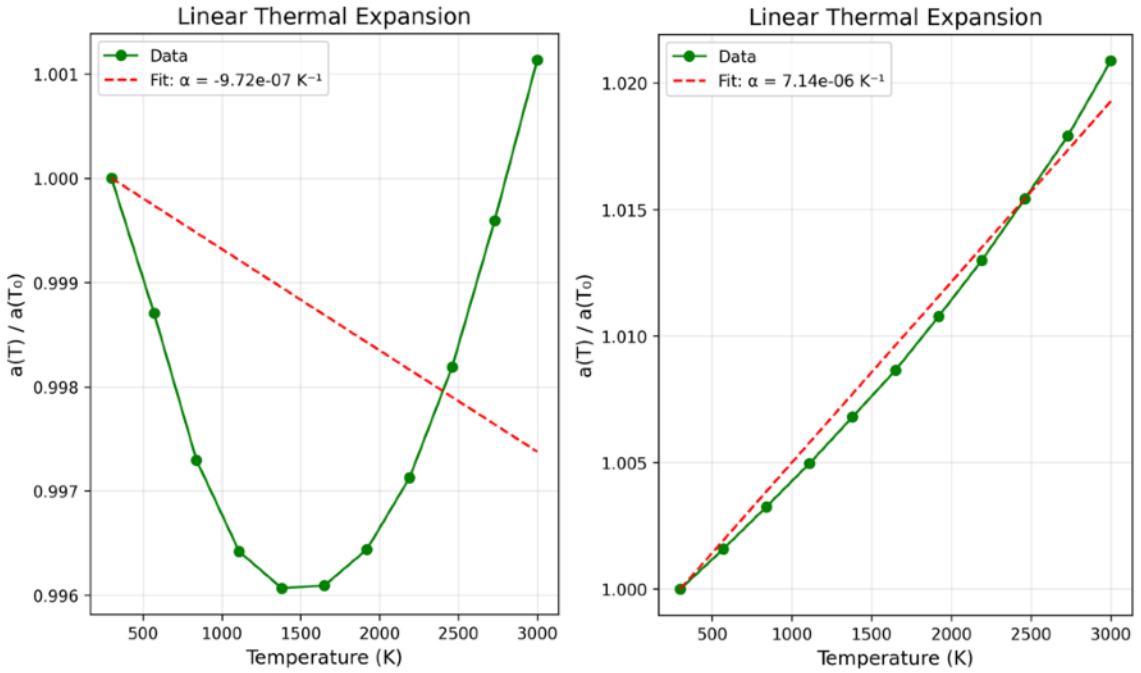

Threshold Displacement Energy

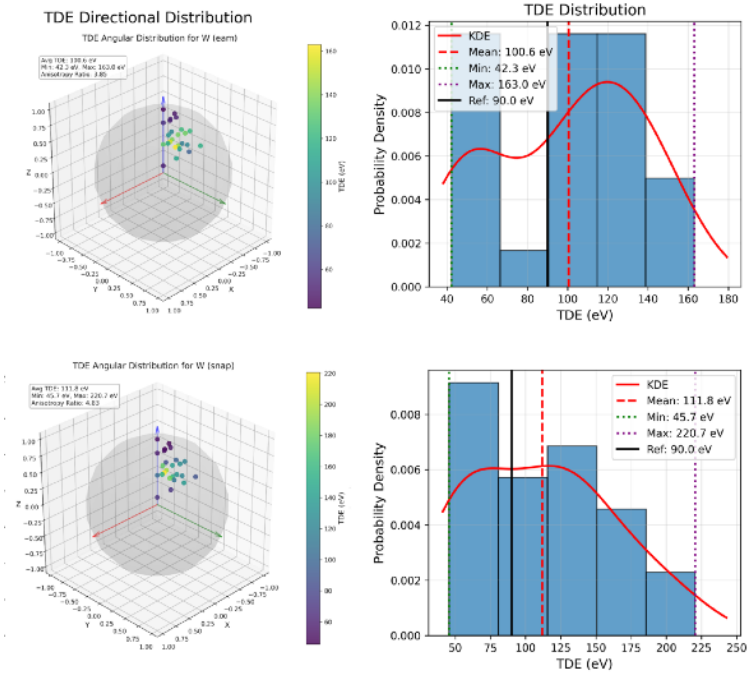

SIA Defect Formation Energies

	Dumbbell <100>	Dumbbell <110>	Dumbbell <111>	Energy Diff. (<111> - <100>)
DND-BN	11.4	9.7	9.4	0.3
WSNAP	11.6	10.4	10.3	0.1

SIA Defect Formation Energies

	Dumbbell <110>	Dumbbell <111>	Energy Diff. (<111> - <100>)	% Rings
DND-BN	9.7	9.4	0.3	0.1
WSNAP	10.4	10.3	0.1	0.6
JW	10	9.6	0.44	0.0
M-S	9.78	9.65	0.1	0.3
tabGap(HEA)	11.28	11.13	0.15	0.1

SIA Defect Formation Energies

	Dumbbell <110>	Dumbbell <111>	Energy Diff. (<111> - <100>)	% Rings
DND-BN	9.7	9.4	0.3	0.1
WSNAP	10.4	10.3	0.1	0.6
test-6	10.1	9.8	0.3	0.1
test-8	9.6	9.3	0.3	0.6
Kanad-S	10.9	10.6	0.3	0.2

Kanad-S: consensus based active learning on configurations extracted from collision cascades

Accuracy on Open Datasets

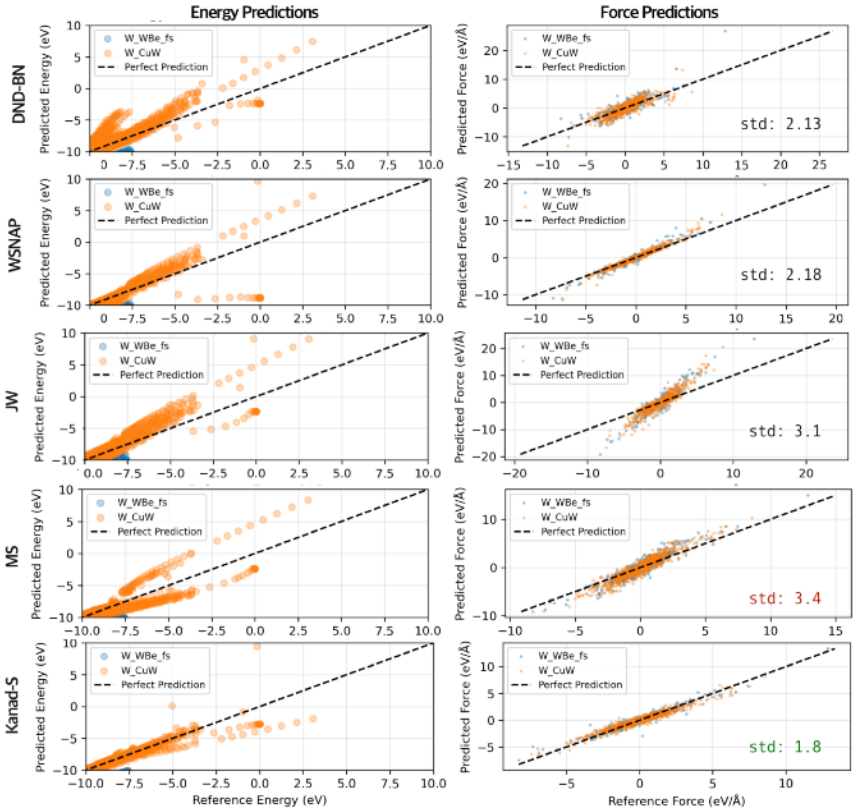

- JW shows slightly different slope deviating more at higher forces.
- Kanad-S shows low deviations but its deviation pattern is different.

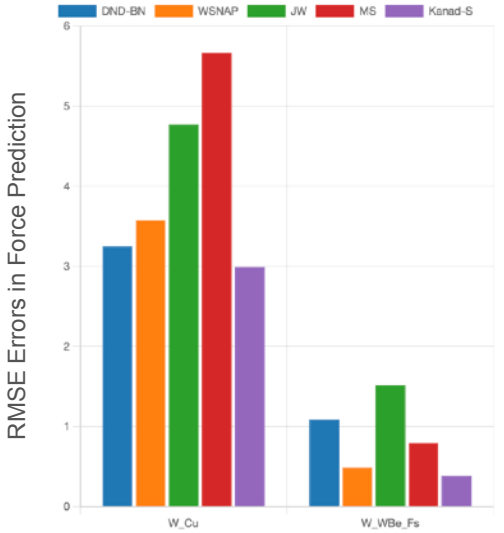

Comparison on Primary Damage Data

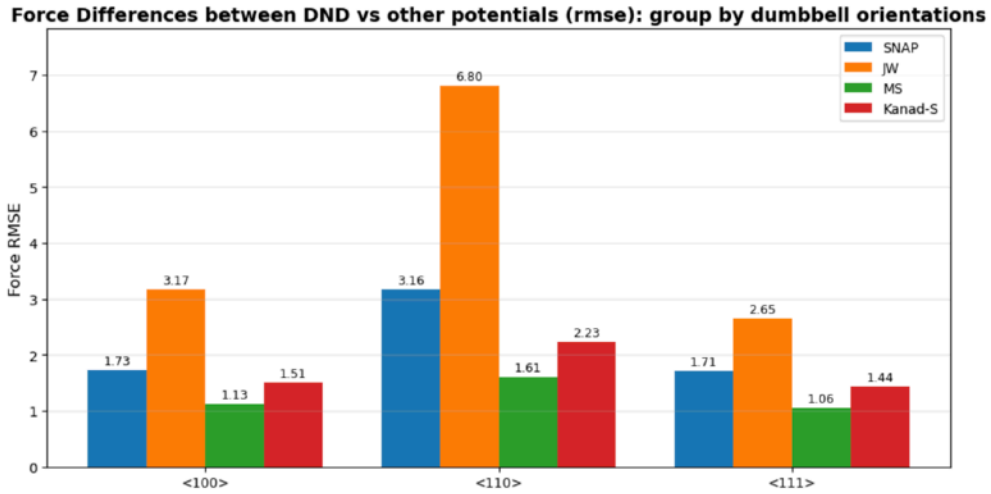

- JW clearly distinguishes itself in <110> and forms no rings.
- MS potential is closest, followed by Kanad-S and SNAP
- Similar to consensus based sampling.

Number of defects & S/R

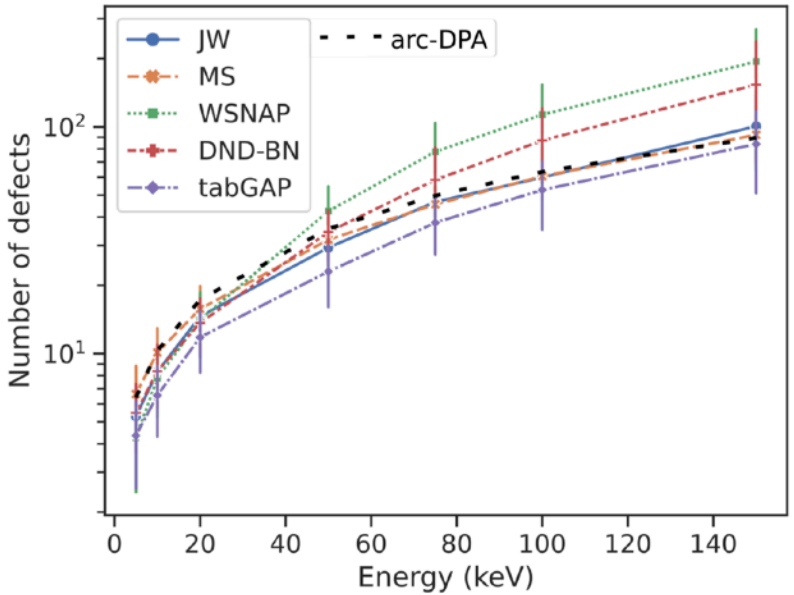

IAP	r1 (Å)	r2 (Å)	R (Å)	S	S/R ($Å^{-1}$)
JW	1.39	2.6	1.4	-150	-107
DND-BN	1.1	2.25	1.3	-230	-177
MS	1.3	2.0	1.45	-137	-95
WSNAP	ZBL	ZBL	1.4	-145	-104
tabGAP	SC	SC	1.27	-223	-176

Table 3: Table of comparison of the five interatomic potentials with experiments and DFT results. The percentage of relative error with respect to either experiments or to DFT, whichever is lesser, is given in brackets. Relative errors in excess of 20 % is made bold-face for easy identification.

Property	DFT	Expt.	JW	MS	DND-BN	WSNAP	tabGAP
a (Å)	3.18	3.17	3.17 (0.15)	3.16 (-0.16)	3.16 (0.0)	3.18 (-0.15)	3.18 (-0.16)
C11 (GPa)	521	522.0	475.33 (-8.77)	517.41 (-0.69)	544.18 (4.25)	538.99 (3.25)	564.87 (8.21)
C12 (GPa)	195	204.0	195.29 (0.15)	7258.66 (**26.79**)	350.89 (**72.01**)	208.73 (2.32)	207.92 (1.92)
C44 (GPa)	147	161.0	154.63 (-3.96)	186.11 (15.59)	242.37 (**50.54**)	152.92 (4.03)	152.15 (3.51)
B (GPa)		310.0	288.64 (-6.89)	344.91 (9.5)	415.32 (**31.85**)	318.82 (1.21)	326.90 (3.78)
S (GPa)		161.0	148.79 (-7.59)	163.42 (1.5)	184.08 (10.89)	157.80 (-1.99)	162.68 (1.04)
ν		0.28	0.29 (4.0)	0.33 (19.03)	0.39 (**40.01**)	0.28 (-0.3)	0.27 (-3.91)
VFE (eV)	3.36	3.80	3.65 (-3.95)	3.86 (1.64)	3.58 (5.91)	3.13 (-6.84)	3.31 (-1.43)
SIA-Oct (eV)	12.27	10.5	10.26 (-2.24)	11.58 (-5.59)	11.53 (-6.06)	12.34 (0.57)	12.23 (-0.34)
SIA-Tet (eV)	11.72	11.2	10.29 (-8.16)	10.88 (-2.9)	10.83 (-3.31)	11.82 (0.84)	12.50 (6.61)
SIA-DB-100 (eV)	12.2	11.5	10.15 (-11.75)	11.87 (-2.7)	11.34 (-1.39)	11.60 (0.87)	12.43 (1.89)
SIA-DB-110 (eV)	10.58	10.60	9.99 (-5.58)	9.78 (-7.59)	9.68 (-8.49)	10.39 (-1.78)	11.28 (6.38)
SIA-DB-111 (eV)	10.29	10.30	9.55 (-7.17)	9.65 (-6.21)	9.37 (-8.98)	10.33 (0.26)	11.14 (8.17)
DB 110-111 (eV)	0.3	0.30	0.44 (**-50.98**)	0.13 (**56.76**)	0.32 (-8.65)	0.06 (**77.81**)	0.13 (**53.69**)
$\alpha(K^{-1})$	4.9e-6	4.5e-6	8.74e-6 (**-78.32**)	5.19e-6 (-5.87)	-9.72e-7 (**119.83**)	7.14e-6 (**-45.72**)	6.79e-6 (**-38.59**)
TDE mean (eV)		90.0	133.79 (**48.65**)	96.79 (7.54)	100.57 (11.75)	111.79 (**24.21**)	109.85 (**22.06**)
TDE max (eV)			249.0	199.70	163.00	220.70	187.70
TDE min (eV)			54.3	43.00	42.30	45.70	38.30
TDE 100 (eV)		42.0	54.30 (**-29.29**)	43.00 (-2.38)	42.30 (-0.71)	45.70 (-8.81)	38.30 (8.81)

Conclusions

- Peripheral point defect number is an important parameter for various properties and shows good dependence on dpa rather than energies & to some extent potentials

- It is easy to find peripheral point defects with efficient geometrical & ML methods where they naturally emerge as more basic.

- The SSC simulations do agree with various experiments with different degree of accuracies depending on MLIP used which is a problem.

- Defect characteristics of primary damage depends on the interplay of multiple parameters and not just single correlations with certain property like s/r, defect formation energies etc.

- Finding reliable signatures for various outcomes with MLIP development rather than iterative validation with expensive MD simulations, experimental comparisons & biases.

- Active learning and consensus based sampling of under-sampled regions is effective in addressing specific issues.

- Standard domain-specific datasets & pre-trained models are promising steps for improving credibility of new MLIPs.

Thank You

Utkarsh Bhardwaj
Email: haptork@gmail.com
BARC - Vizag, India